In Vivo Detection of Intervertebral Disk Injury Using a Radiolabeled Monoclonal Antibody Against Keratan Sulfate

Kalevi J.A. Kairemo, Anu K. Lappalainen, Eeva Kääpä, Outi M. Laitinen, Timo Hyytinen, Sirkka-Liisa Karonen, and Mats Grönblad

Departments of Clinical Chemistry, Physical Medicine and Rehabilitation, and Thoracic and Cardiovascular Surgery, Helsinki University Central Hospital, Helsinki; and Faculty of Veterinary Medicine, Department of Clinical Veterinary Sciences, University of Helsinki, Helsinki, Finland

In the intervertebral disk, proteoglycans form the major part of the extracellular matrix, surrounding chondrocytelike disk cells. Keratan sulfate is a major constituent of proteoglycans. **Methods:** We have radioiodinated a monoclonal antibody raised against keratan sulfate. This antibody was injected into rats (n = 6), and the biodistribution was studied. A model of intervertebral disk injury was developed, and two tail disks in each animal with both acute (2 wk old) and subacute (7 wk old) injuries were studied for in vivo antibody uptake. **Results:** The biodistribution at 72 h was as follows: blood, 0.0018 percentage injected dose per gram of tissue (%ID/g); lung, 0.0106 %ID/g; esophagus, 0.0078 %ID/g; kidney, 0.0063 %ID/g; liver, 0.0047 %ID/g; spleen, 0.0046 %ID/g; heart, 0.0036 %ID/g; thyroid, 0.0034 %ID/g; muscle, 0.0017 %ID/g; and bone, 0.0016 %ID/g. In the subacute stage, a significant difference ($P < 0.006$) was found in antibody uptake between injured disks (n = 12) and adjacent healthy disks (n = 12). In vivo γ imaging showed increased uptake in other animals having lumbar disk injuries (2, 7, and 17 d after injury). Cartilage tissue, such as the trachea, was studied separately and showed extremely high antibody uptake, 0.10 %ID/g. Rat trachea was also visualized on γ images. **Conclusion:** Our data suggest that antibodies against nucleus pulposus components, such as proteoglycans, can be used for in vivo detection of intervertebral disk injury. This finding is in spite of the minimal circulation present in intervertebral disks.

Key Words: monoclonal antibodies; keratan sulfate; disk injury; intervertebral disk; cartilaginous tissue; radioimmunodetection

J Nucl Med 2001; 42:476–482

Intervertebral disk pathology may be shown clinically either by MRI, with or without contrast enhancement, or by diskography. In more recent studies, MRI has been used for revealing a high-intensity zone in the posterior peripheral rim of the intervertebral disk, a radiologic finding that has been suggested to be related to back pain (*1*,*2*). None of the present in vivo methods, however, show more detailed pathology coupled with intervertebral disk degeneration or disk injury. In particular, at present no reliable in vivo methods are available for revealing annulus fibrosus pathology.

If successful, specific in vivo targeting of the intervertebral disk by labeled antibodies, directed to specific molecular structures, will provide clinicians with a means for studying mechanisms of disk pathology. The ability to follow in vivo reparative and degenerative processes prospectively may also become possible. In comparison, MRI can be considered a coarse method for studying intervertebral disk pathophysiology, even though the method has certain advantages such as noninvasiveness and lack of exposure to radiation. However, clearly needed is the development of more specific diagnostic methods in this respect.

Serum keratan sulfate levels have in several studies been reported to be related to degenerative changes in cartilaginous tissue (*3*). In addition, massive and rapid degradation of intervertebral disks was determined to result in a large rise in serum keratan sulfate levels (*3*).

More detailed immunohistochemical analysis of an articular disk has shown that keratan sulfate is associated with the large chondroitin sulfate proteoglycan concentrating inside and away from the periphery of the structure but close to the inferior and superior surfaces (*4*). This type of distribution may reflect the adaptation of the extracellular matrix to mechanical stress (*4*). This possibility has been studied experimentally by inducing surgically articular disk displacement; in an animal study, sulfated glycosaminoglycans, such as keratan sulfate, chondroitin-4-sulfate, and chondroitin-6-sulfate, showed immunohistochemical reduction in the articular disk at 2 wk after induction of disk displacement (*5*). At 6 wk, the immunostaining sulfated glycosaminoglycans increased (*5*). Figure 1 illustrates the structural relationships of keratan sulfate and chondroitin sulfates in an intervertebral disk. Clinically, disk pathology is usually found to be caused by a prolonged process of

Received Jun. 6, 2000; revision accepted Sep. 14, 2000.

For correspondence or reprints contact: Kalevi J.A. Kairemo, MD, PhD, Department of Nuclear Medicine, Helsinki University Central Hospital, P.O. Box 340, FIN-00290 Helsinki, Finland.

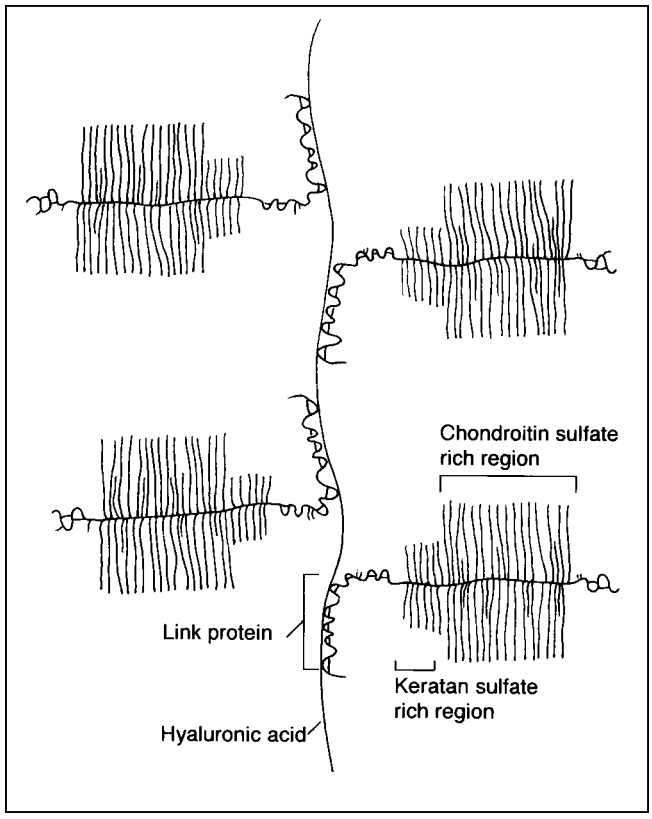

FIGURE 1. Schematic diagram shows proteoglycan molecule and structural relationships between two main moieties, keratan sulfate and chondroitin sulfate. In intervertebral disk, proteoglycans form major part of extracellular matrix, surrounding chondrocytelike disk cells. Keratan sulfate was target molecule for studying experimental intervertebral disk injury in rats.

intervertebral disk degeneration, which is to a large extent genetically determined (*6–8*). However, some investigators (*9*) have suggested that traumatic rim lesions of the disk may result in disk degeneration as well, and the suggestion is supported by results from several studies of animal models of intervertebral disk injury. As a result of the peripheral disk lesion, intervertebral disk degeneration eventually develops and has many similarities to human disk degeneration (*9,10*). Consequently, models of intervertebral disk injury using a stab incision have been employed by many investigators on rabbit (*11,12*), ovine (*9,13*), and porcine (*10,14*) disks. So far, no model of intervertebral disk injury has been established in rats, but as early as 50 y ago, Lindblom (*15*) observed signs of disk degeneration after several weeks of U-shaped immobilization of the rat tail.

Peripheral disk injuries may be highly relevant clinically with respect to mechanisms of low back pain, because only the most peripheral part of the intervertebral disk is normally innervated, whereas the deeper parts are both aneural and avascular (*16*). As far as we are aware, stab incision models of intervertebral disk injury in rats have not been studied. In this study, we introduced a model of simultaneous stab incisions to rat tail and lumbar spine disks. Our study sought to determine the feasibility of using a specific radiolabeled antibody for studying experimental intervertebral disk injury. We sought to determine whether such a method would show altered, possibly increased, uptake after a stab lesion to the disk and whether the method would be sensitive enough for visualizing such an injury. We included injuries of lumbar spine disks in our investigation because injection into the tail vein, which is close to the tail disks, may theoretically produce nonphysiologic uptake of the radiolabeled antibody in tail disks.

To our knowledge, no studies have been performed on the distribution of sulfated glycosaminoglycans in a model of intervertebral disk injury. Therefore, we developed such a model that can be used for studying the distribution pattern of keratan sulfate. Another aim of this study was to test the model for in vivo detection of disk injury using radiolabeled monoclonal antibodies (MAbs) against nucleus pulposus components.

MATERIALS AND METHODS

MAb Characteristics

An IgG_{2b} subclass mouse MAb (clone EFG-11; Serotec Ltd., Kidlington, U.K.) raised against human adult cartilage proteoglycans was used. This antibody, which is known to cross-react with rat cartilage keratan sulfate, also reacts with fetal type cartilage proteoglycans and cross-reacts with human, bovine, rabbit, canine articular, and chicken sternal cartilage proteoglycans (*17*). As a control in imaging studies, a rabbit polyclonal antibody against rat type III collagen was used (reference number 10341; Laboratoire de Pathologie Cellulaire, Institut Pasteur de Lyon, Lyon, France).

Labeling of Antibodies

With solid lactoperoxidase, 500 μg MAb (10 mg/mL) were iodinated with 75 MBq Na-^{125}I (Amersham, Little Chalfont, U.K.) (*18*). The solid lactoperoxidase was prepared as follows. Fifteen milligrams of B-grade lactoperoxidase (EC 1.11.1 0.8) (Calbiochem, La Jolla, CA) were coupled to 100 mg of the copolymer of maleic acid anhydride and butanediol divinylether (E. Merck, Darmstadt, Germany). The lactoperoxidase suspension was first diluted 1:5 with 0.1 mol/L sodium acetate buffer, pH 6.0. The iodination was started by adding radioiodine and 20 μL hydrogen peroxide, 0.88 mmol/L, followed by two 10-μL additions of hydrogen peroxide during 30 min. Thereafter, purification was performed using size-exclusion chromatography with PD-10 columns (Sephadex 25G; Pharmacia, Uppsala, Sweden) equilibrated with a tiny amount of 1% bovine serum albumin–phosphate buffer (0.05 mol/L).

One-milliliter fractions were eluted with isotonic sodium chloride. The labeling efficiency was tested with thin-layer chromatography (ITLC SG; Gelman Sciences, Ann Arbor, MI) using acetone as the eluent. Appropriate labeling was confirmed by cutting the strips to pieces and counting them in a γ counter (LKB 1282 CompuGamma; Wallac Oy, Turku, Finland). The control antibody against rat type III collagen was labeled using the same procedure.

Surgery Model

Healthy male Wistar rats 12 wk old and weighing approximately 400 g were used. The animals were anesthetized with

medetomidine (Domitor, 1 mg/mL injection; Orion, Espoo, Finland), 500 μg/kg subcutaneously, and ketamine hydrochloride (Ketalar, 50 mg/mL; Parke-Davis, Solna, Sweden), 25 mg/kg intraperitoneally. For tail injuries, the animals were placed in sternal recumbence. A stab incision using a number 11 scalpel was made in two adjacent proximal tail disks. Prolapsed disk material was seen every time. For lumbar disk injuries, the animals were placed in dorsal recumbence. One stab incision in the annulus of the disk was done in each animal intraperitoneally using a number 11 scalpel. Prolapsed disk material was not seen during the operation. All the injury sites were marked with nonabsorbable suture material. Wounds were closed routinely. Buprenorfin hydrochloride (Temgesic, 0.3 mg/mL injection; Reckitt and Coleman, Hull, England), 0.15 mg/kg, was given subcutaneously for pain relief postoperatively and then two times per day for 2 d.

Biodistribution Model

Healthy male Wistar rats weighing approximately 400 g were used. The injuries were 2 wk old in acute and 7 wk old in subacute biodistribution studies. Under general anesthesia with medetomidine and ketamine hydrochloride, each animal received an intravenous tail-vein injection of 2.44–4.00 MBq radioactivity containing approximately 100 μg antikeratan sulfate MAb. The animals also received 0.1 mL 5% potassium iodide to block the thyroid because of possible in vivo dehalogenation of the radioiodinated antibody. The animals were killed 72 h after each radioantibody injection ($n = 6$). An aliquot of the injected dose was measured; the organs and tissues (lung, heart, kidney, liver, spleen, trachea, bone, muscle, and blood) were isolated, washed, and weighed; and the radioactivity of each isolated tissue was measured using a γ counter. The data were calculated as percentage of injected dose per gram of tissue (%ID/g). Similarly, the tail disks were isolated, and both acute ($n = 12$) and subacute ($n = 12$) lesions were analyzed. The findings were compared with those of healthy adjacent disks.

In Vivo Imaging

Additionally, three male Wistar rats weighing approximately 400 g were studied using γ imaging. These animals had both lumbar and tail disk injuries, which were 2, 7, and 17 d old before radioantibody injection. Anesthetized animals were imaged at 24 and 96 h after injection using a 1500 XP gamma camera (Picker International Inc., Highland Heights, OH) equipped with a low-energy ultra-high-resolution collimator (γ-energy peak, 30 keV; 35% window). The matrix size was 256 × 256 × 16. The animals were supine, and a minimum of 500,000 counts was collected. Imaging took approximately 20 min.

This study was performed with the permission of the ethical committees for animal studies of Helsinki University Central Hospital and the Faculty of Veterinary Medicine of the University of Helsinki and with the permission of the County Administration Board of Southern Finland.

RESULTS

We have radioiodinated a mouse MAb raised against keratan sulfate cross-reacting with rat tissues. The labeling yield after lactoperoxidase solid iodination was always low, approximately 50%–60%, and purification with gel filtration was needed. The labeling efficiencies in the purified products varied from 80% to 95%, and labeling efficiencies higher than 90% seen on instant thin-layer chromatography were used only for in vivo studies.

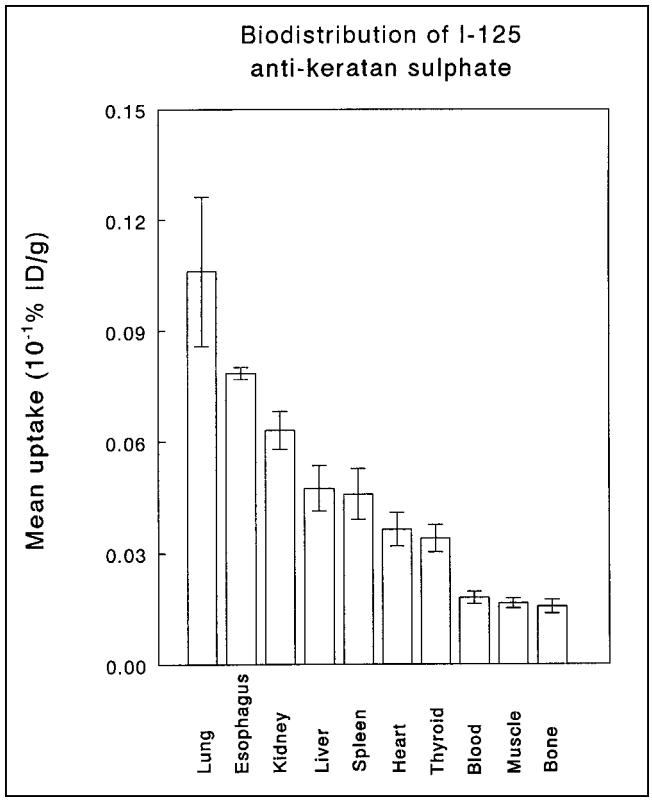

FIGURE 2. Biodistribution after intravenous injection of ^{125}I-labeled MAb against keratan sulfate at 72 h. Error bars stand for SD.

The biodistribution data at 72 h in different organs are presented in Figure 2. The observed uptakes were 0.0018 %ID/g in blood, 0.0106 %ID/g in lung, 0.0078 %ID/g in esophagus, 0.0063 %ID/g in kidney, 0.0047 %ID/g in liver, 0.0046 %ID/g in spleen, 0.0036 %ID/g in heart, 0.0034 %ID/g in thyroid, 0.0017 %ID/g in muscle, and 0.0016 %ID/g in bone. These data show that most of the activity from the major organs had been cleared out and the thyroid activity was low. The highest activity was seen in the lung. A detailed biodistribution of thoracic organs is presented in Figure 3. The highest activity was seen in trachea, 0.10%. The trachea-to-esophagus ratio was 12.8, and the trachea-to-lung ratio was 9.4. Uptake in the model of intervertebral disk injury is presented in Figure 4. The data are presented separately for both acute (2 wk) and subacute (7 wk) lesions, and uptake in the disks was close to that in major organs (kidney, liver, spleen, and heart). A clearly significant difference was seen in antibody uptake between injured disks ($n = 12$) and adjacent healthy disks ($n = 12$) in subacute injury ($P < 0.006$, Wilcoxon matched-pairs test, Fig. 4). In acute injury, the difference between injured disks ($n = 12$) and adjacent healthy disks ($n = 12$) was not statistically significant ($P = 0.27$, Wilcoxon matched-pairs test, Fig. 4).

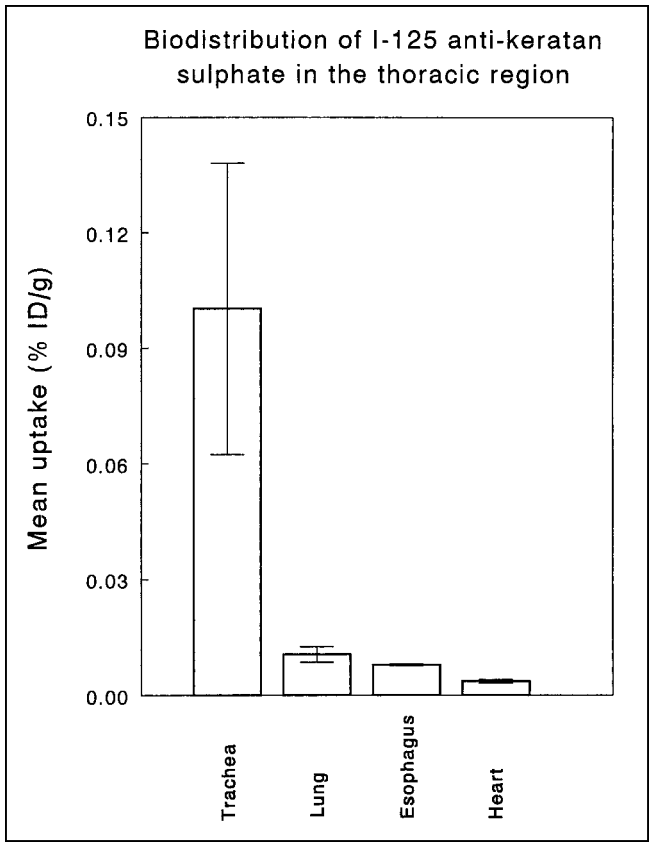

FIGURE 3. Biodistribution in detail in thoracic organs after intravenous injection of ^{125}I-labeled MAb against keratan sulfate at 72 h. Error bars stand for SD.

Figure 5 shows in vivo γ images obtained 4 d after MAb injections in animals with lumbar and tail disk injuries (2, 7, and 17 d old). Increased uptake was seen in the lumbar lesion in animals with 7- and 17-d-old injuries (Fig. 5, middle and right). The tail disk injuries were also localized in the animals with 7- and 17-d-old injuries. In the animal with a 2-d-old injury, no uptake occurred in the lesions (Fig. 5, left). The trachea was also seen but was masked by high thyroid uptake. Figure 6 shows three other animals with lumbar and tail disk injuries (2, 7, and 17 d old) who received injections of control antibody against rat collagen III. No uptake occurred in the lesions. The trachea was not seen in these animals.

DISCUSSION

To our knowledge, in vivo labeling techniques have not yet been applied as in this study. However, indirect ^{35}S-sulfate incorporation into proteoglycans of intervertebral disks in beagles and greyhounds has been measured (*19*).

The same technique can be used for cell cultures. For example, the rate of ^{35}S-sulfate incorporation into proteoglycans, and the contents of various extracellular matrix molecules (total sulfated proteoglycans, antigenic keratan sulfate, hyaluronan, collagen, and pyridinium cross-links) have been measured (*20*). In these prior studies, nucleus pulposus cells synthesized fewer proteoglycan and collagen molecules and were less effective than annulus fibrosus cells in incorporating these into the cell-associated matrix, a protective shell rich in proteoglycans and collagen molecules. Nucleus pulposus cells are extremely sluggish in reforming a cell-associated matrix (*20*). This sluggishness may explain why damage to the nucleus pulposus often is accompanied by progressive degeneration of the disk in vivo (*20*).

In spite of minimal circulation in the annulus fibrosus and nucleus pulposus, we have been able to show in vivo targeting by radiolabeled antibody in injured intervertebral disks. Our data suggest that antibodies against nucleus pulposus structures, such as proteoglycans and, particularly, keratan sulfate, can be used for in vivo detection of intervertebral disk injury. The conditions for in vivo detection were difficult because of the size of the rat disk. It is not much bigger than a reasonable pixel size for imaging studies, which is 2.3 × 2.3 mm in Figure 5.

Therefore, γ counting for absolute antibody uptake had to be performed. The differences were significant between the injured disks and the adjacent healthy disks, but only for subacute lesions. In the acute stage, differences in uptake in injured and control disks did not reach a level of statistical significance. This type of lesion should allow antibodies to migrate to the nucleus pulposus more easily, because circulation is normally lacking. The antibody penetration in the tissue is caused by diffusion, as regulated by the interstitial fluid pressure, and is thus slow (*21*). With annulus fibrosus injury, the distance to the nucleus pulposus, where keratan sulfate is mostly located, becomes shorter.

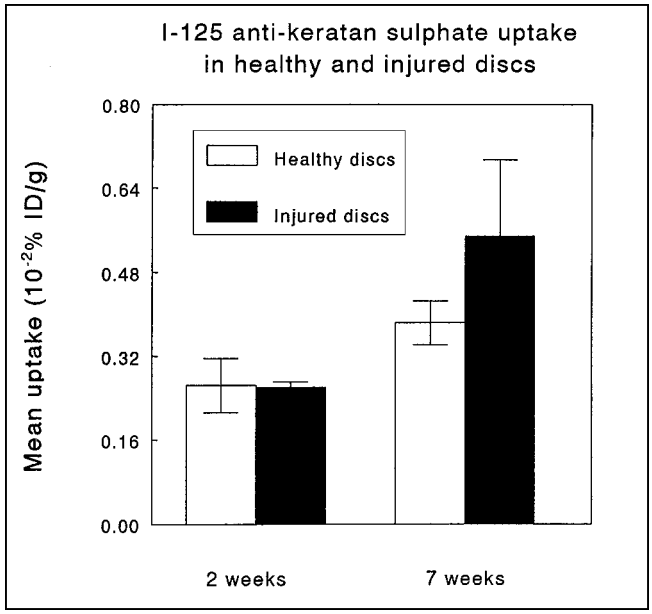

FIGURE 4. Biodistribution in acute (2 wk) and subacute (7 wk) lesions after intravenous injection of ^{125}I-labeled MAb against keratan sulfate at 72 h. Error bars stand for SD. Difference between healthy and injured disks in subacute lesions was statistically significant ($P < 0.006$).

FIGURE 5. γ images 4 d after injection of ^{125}I-labeled MAb against keratan sulfate in animals with both lumbar and tail disk injuries (injuries are 2 d old on left, 7 d old in middle, and 17 d old on right). Increased uptake in lumbar lesion in animals with 7- and 17-d-old injuries (solid arrows) is best seen in middle in lower back. Lesion size was approximately 2 × 2 mm. Similarly, tail disk injuries are localized in animals with 7- and 17-d-old injuries (solid arrows). Injection sites are seen (open arrows) in these animals and make tail uptake diffuse in animal with 7-d-old injury (no arrows). In animal with 2-d-old injury, lesions show no uptake. Tracheas were also visualized but, unfortunately, are masked here by high thyroid uptake because these animals were not blocked for thyroid.

MAbs have been used for determining the distribution of various components of the proteoglycan molecule in the intervertebral disk and cartilage endplate (22). The degree of immunoreactivity varies with location, being greater in the nucleus pulposus than in the annulus fibrosus, with least reactivity in the cartilage endplate (*22*). Many antibodies against keratan sulfates from articular cartilage, intervertebral disks, and cornea have been described; for example, MAbs 3D12/H7 and 5D4 show different immunochemical reactivity for different keratan sulfates (*23*). Four other MAbs (designated AC2, AH12, DB10, and DD11) derived from mice immunized with the large chondroitin sulfate proteoglycan from the bovine temporomandibular joint disk recognize keratan sulfate (*4*).

In cell cultures, intervertebral disk proteoglycans have been shown to contain low amounts of keratan sulfate—less than 5% of the total glycosaminoglycans synthesized (*24*). The chondroitin sulfates are more abundant in all zones of the disk, with chondroitin 4-sulfate accounting for 29%–39% and chondroitin-6-sulfate accounting for 51%–67% (*24*). Antibodies against these proteoglycans may also be used in vivo. The chemical morphology of human intervertebral disk glycosaminoglycans of nucleus pulposus and annulus fibrosus depends on the origin, that is, cervical, thoracic, or lumbar (*25*). There are also age-related changes. In a study of disk samples from patients aged 36–79 y, keratan sulfate increased in all disks with increasing maturity. Oversulfated keratan sulfate, absent from fetal disks, reached mature levels by 10 y, and increased keratan sulfate–to–chondroitin sulfate ratios before maturity correlated with decreased disk blood supply (*25*).

Intervertebral disks contain several phenotypically different chondrocytic cell populations; this fact has been shown in cell cultures from adult human nondegenerative nucleus pulposus and annulus fibrosus (*26*). The majority of the cells (>60%) from both the annulus fibrosus and the nucleus pulposus produced both keratan sulfate and chondroitin sulfate (*26*). In a rat model, the development of fibrocartilage in lumbar intervertebral disks has been studied by immunohistochemistry (*27*). In late phases, tissue differentiation was characterized by the appearance of type II collagen, chondroitin 4-sulfate, and keratan sulfate in the inner

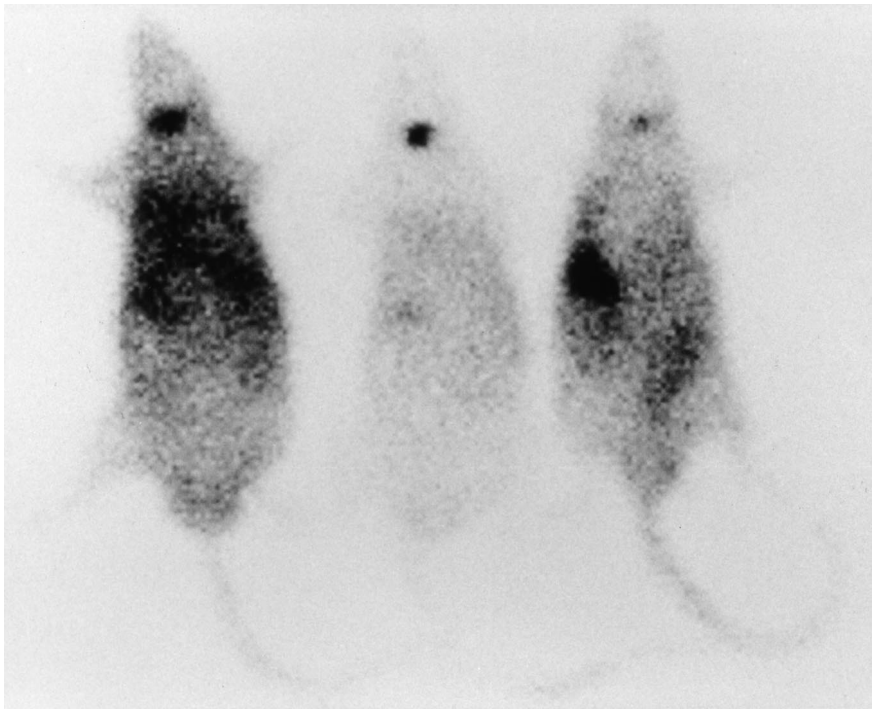

FIGURE 6. γ images 4 d after injection of ^{125}I-labeled MAb against rat collagen III in animals with both lumbar and tail disk injuries (injuries are 2 d old on left, 7 d old in middle, and 17 d old on right). Lesions show no uptake. Trachea was not visualized in these animals.

annulus. These components also appeared in the outer annulus, but only in adult animals (*27*). Keratan sulfate has been shown to functionally replace chondroitin sulfate in conditions of low oxygen (*28*). The critical electrolyte concentration in both the annulus and the nucleus of cervical, thoracic, and lumbar intervertebral disks distinguished three age-related groups: less than 3 mo; from 3 mo to 5 y, and more than 10 y (*28*).

This study introduced a model that used a stab incision into a rat tail disk. Our rat tail model offers easy access to intervertebral disks. Difficulties, however, may arise from the small size of the disk. We observed significantly increased uptake of the keratan sulfate label only in the 7-wk subacute stage, not in the 2-wk acute stage. This finding may have been caused by a proportional increase of keratan sulfate with time after the injury. In another study, in which the rabbit craniomandibular joint was used as a model for disk displacement, an observable decrease in the tissue concentration of keratan sulfate occurred at 2 wk, and an increase occurred at 6 wk (*5*).

The mean uptakes that we observed at 72 h in the disks, $0.26-0.55 \times 10^{-2}$ %ID/g (Fig. 4), were close to those of major organs such as the kidney, liver, spleen, and heart (Fig. 2). This finding indicates that most of the activity had been cleared from major organs at that time, whereas uptake was increased as a function of time in the cartilage tissue because of poor blood supply. This may open up possibilities for clinical applications with other specific antibodies raised against human antigens. Recently, the avidin/^{111}In-biotin approach was used for imaging inflammatory foci in orthopedic patients (*29*). In that study, the authors could show intervertebral disk lesions with a nonspecific tracer using ^{111}In as a radionuclide. Our antibody labeled with ^{123}I may be suitable clinically. Unfortunately, the targeting process itself is slow, and the half-life of ^{123}I may thus be too short. One option is to use a multiple-step targeting approach based on avidin/biotin amplification. Then it would be easiest to inject a specific biotinylated MAb against nucleus pulposus structures and afterwards, when all the nonspecifically bound MAb has been cleared out, to inject a labeled avidin to localize the preinjection specifically bound MAb.

CONCLUSION

Our data suggest that antibodies against nucleus pulposus components, such as proteoglycans, can be used for in vivo detection of intervertebral disk injury. This is a new field in nuclear medicine and clinically important in, for example, the evaluation of low back pain. Surprisingly, significant differences in damaged and healthy intervertebral disks were observed using a labeled MAb against keratan sulfate in spite of minimal circulation in the cartilage tissue.

REFERENCES

1. Saifuddin A, Braithwaite I, White J, Taylor BA, Renton P. The value of lumbar spine magnetic resonance imaging in the demonstration of annular tears. *Spine*. 1998;23:453–457.
2. Schellhas KP, Pollei SR, Gundry CR, Heithoff KB. Lumbar high-intensity zone: correlation of magnetic resonance imaging and discography. *Spine*. 1996;21:79–86.
3. Kuiper JI, Verbeek JH, Frings-Dresen MH, Ikkink AJ. Keratan sulfate as a potential biomarker of loading of the intervertebral disc. *Spine*. 1998;23:657–663.
4. Nakano T, Imai S, Koga T, Dodd CM, Scott PG. Monoclonal antibodies to the large chondroitin sulphate proteoglycan from bovine temporomandibular joint disc. *Matrix*. 1993;13:243–254.

5. Ali AM, Sharawy M. Histochemical and immunohistochemical studies of the effects of experimental anterior disc displacement on sulfated glycosaminoglycans, hyaluronic acid, and link protein of the rabbit craniomandibular joint. *J Oral Maxillofac Surg*. 1996;54:992–1003.
6. Annunen S, Paassilta P, Lohiniva J, et al. An allele of COL9A2 associated with intervertebral disc disease. *Science*. 1999;285:409–412.
7. Kawaguchi Y, Osada R, Kanamori M, et al. Association between an aggrecan gene polymorphism and lumbar disc degeneration. *Spine*. 1999;24:2456–2460.
8. Kimura T, Nakata K, Tsumaki N, et al. Progressive degeneration of articular cartilage and intervertebral discs: an experimental mutation. *Int Orthop*. 1996; 20:177–181.
9. Osti OL, Vernon-Roberts B, Fraser RD. 1990 Volvo Award in experimental studies: anulus tears and intervertebral disc degeneration—an experimental study using an animal model. *Spine*. 1990;15:762–767.
10. Kääpä E, Holm S, Inkinen R, Lammi M, Tammi M, Vanharanta H. Proteoglycan chemistry in experimentally injured porcine intervertebral disc. *J Spinal Disord*. 1994;7:296–306.
11. Smith JW, Walmsley STA. Experimental incisions of the intervertebral disc. *J Bone Joint Surg Br*. 1951;33-B:612–625.
12. Lipson SJ, Muir H. Vertebral osteophyte formation in experimental disc degeneration. *Arthritis Rheum*. 1980;23:319–324.
13. Melrose J, Ghosh P, Taylor TKF, et al. A longitudinal study of the matrix changes induced in the intervertebral disc by surgical damage to the annulus fibrosus. *J Orthop Res*. 1992;10:665–676.
14. Keller TS, Hansson TH, Holm SH, Pope MM, Spengler DM. *In vivo* creep behavior of the normal and degenerated porcine intervertebral disk: a preliminary report. *J Spinal Disord*. 1989;1:267–278.
15. Lindblom K. Experimental ruptures of intervertebral discs in rat tails. *J Bone Joint Surg Am*. 1952;34-A:123–128.
16. Palmgren T, Grönblad M, Virri J, Kääpä E, Karaharju E. An immunohistochemical study of nerve structures in the anulus fibrosus of human normal lumbar intervertebral discs. *Spine*. 1999;24:2075–2079.
17. Caterson B, Christner JE, Baker JB. Identification of a monoclonal antibody that specifically recognizes corneal and skeletal keratan sulphate. *J Biol Chem*. 1983;258:8843–8854.
18. Karonen S-L, Mörsky P, Siren M, Seuderling U. An enzymatic solid-phase method for trace iodination of proteins and peptides with iodine-125. *Anal Biochem*. 1975;67:1–10.
19. Ghosh P, Melrose J, Cole TC, Taylor T. A comparison of the high buoyant density proteoglycans isolated from the intervertebral discs of chondrodystrophoid and non-chondrodystrophoid dogs. *Matrix*. 1992;12:148–155.
20. Chiba K, Andersson GB, Masuda K, Thonar EJ. Metabolism of the extracellular matrix formed by intervertebral disc cells cultured in alginate. *Spine*. 1997;22: 2885–2893.
21. Jain RK. Vascular and interstitial barriers to delivery of therapeutic agents in tumors. *Cancer Metastasis Rev*. 1990;9:253–266.
22. Roberts S, Caterson B, Evans H, Eisenstein SM. Proteoglycan components of the intervertebral disc and cartilage endplate: an immunolocalization study of animal and human tissues. *Histochem J*. 1994;26:402–411.
23. Fischer DC, Haubeck HD, Eich K, et al. A novel keratan sulphate domain preferentially expressed on the large aggregating proteoglycan from human articular cartilage is recognized by the monoclonal antibody 3D12/H7. *Biochem J*. 1996;318:1051–1056.
24. Maldonado BA, Oegema TR Jr. Initial characterization of the metabolism of intervertebral disc cells encapsulated in microspheres. *J Orthop Res*. 1992;10: 677–690.
25. Scott JE, Bosworth TR, Cribb AM, Taylor JR. The chemical morphology of age-related changes in human intervertebral disc glycosaminoglycans from cervical, thoracic and lumbar nucleus pulposus and annulus fibrosus. *J Anat*. 1994; 184:73–82.
26. Chelberg MK, Banks GM, Geiger DF, Oegema TR Jr. Identification of heterogeneous cell populations in normal human intervertebral disc. *J Anat*. 1995;186: 43–53.
27. Rufai A, Benjamin M, Ralphs JR. The development of fibrocartilage in the rat intervertebral disc. *Anat Embryol (Berl)*. 1995;192:53–62.
28. Taylor JR, Scott JE, Cribb AM, Bosworth TR. Human intervertebral disc acid glycosaminoglycans. *J Anat*. 1992;180:137–141.
29. Lazzeri E, Manca M, Molea N, et al. Clinical validation of the avidin/indium-111 biotin approach for imaging infection/inflammation in orthopaedic patients. *Eur J Nucl Med*. 1999;26:606–614.